

12p

N63-1528j  
Code 1

*Technical Report No. 32-131*

*The Perturbations of a Hyperbolic  
Orbit by an Oblate Planet*

*Carl G. Sauer, Jr.*

OTS PRICE

XEROX        \$ 1.60 ph  
MICROFILM   \$ 0.80 mf

-----



JET PROPULSION LABORATORY  
CALIFORNIA INSTITUTE OF TECHNOLOGY  
PASADENA, CALIFORNIA

January 15, 1963

NATIONAL AERONAUTICS AND SPACE ADMINISTRATION  
CONTRACT No. NAS 7-100

*Technical Report No. 32-131*

*The Perturbations of a Hyperbolic  
Orbit by an Oblate Planet*

*Carl G. Sauer, Jr.*



---

C. Gates, Chief  
Systems Analysis Section

JET PROPULSION LABORATORY  
CALIFORNIA INSTITUTE OF TECHNOLOGY  
PASADENA, CALIFORNIA

January 15, 1963

Copyright © 1963  
Jet Propulsion Laboratory  
California Institute of Technology

The material in this Report appeared in the *ARS Journal*, Vol. 32, No. 5, pp. 714-717.

## CONTENTS

I. Introduction . . . . .	1
II. The Perturbative Potential . . . . .	2
III. Variation of the Orbital Elements . . . . .	2
IV. Example of an Earth-Escape Mission . . . . .	4
References . . . . .	8

## TABLES

1. Example of an Earth-escape mission . . . . .	5
2. Asymptotic value of the orbital elements . . . . .	5
3. Asymptotic perturbations of the hyperbolic excess velocity vector . . . . .	6
4. Calculated and observed perturbations at 240 min . . . . .	6
5. Position and velocity at $T = 240$ min . . . . .	7

## FIGURES

1. Perturbation of the semi-transverse axis . . . . .	5
2. Perturbation of the eccentricity . . . . .	5
3. Perturbation of the time of peri-focal passage . . . . .	6
4. Perturbation of the inclination . . . . .	6
5. Perturbation of the argument of perigee . . . . .	6
6. Perturbation of the longitude of the ascending node . . . . .	7
7. True anomaly vs time ( $e = 1.25$ ) . . . . .	7

**ABSTRACT**

15281

The perturbations of the hyperbolic orbital elements of a vehicle in the gravitational field of an oblate planet are derived as functions of the initial osculating elements. Assumptions are made that atmospheric drag is absent and that the gravitational potential of the planet may be represented adequately by the principal term and the second harmonic. An example of an Earth-escape mission is presented in which a comparison is made between calculated orbital perturbations and results from a numerical integration of the equations of motion.

**I. INTRODUCTION**

Although the variations of the orbital elements of Earth satellites have been derived numerous times, nevertheless a treatment of the variation of the orbital elements of a vehicle for an escape mission is lacking except for the case of perturbed hyperbolic motion in the equatorial plane (see Ref. 1).<sup>1</sup> There are several instances in which the results of this paper are of interest, the first being the perturbations of the escape hyperbola from Earth of a lunar or interplanetary probe, and the second being the

perturbations of an interplanetary probe by an oblate planet at encounter.

<sup>1</sup>Since 1960, when this report was originally prepared, there have been two additional papers published concerning the perturbing effects of an oblate planet upon a vehicle on a hyperbolic trajectory (Ref. 2 and 3). Of particular interest is Ref. 3 by G. Hori in which the Von-Zeipel method was used to derive the perturbed motion. The present paper uses the method of Poisson-LaGrange, as does Ref. 2.

## II. PERTURBATIVE POTENTIAL

If an axially symmetric density distribution of the planet is assumed, the gravitational potential function  $U$  may be expanded in terms of surface zonal harmonics of the form (Ref. 4 and 5).

$$U = \frac{k^2}{r} \left[ 1 - \sum_{p=2}^{\infty} J_p r^p P_p(\sin \phi) \right] \quad (1)$$

where

- $J_p$  = the coefficients of the zonal harmonics  $P_p(\sin \phi)$
- $k^2 = GM$  = gravitational constant of attracting body
- $r$  = radial distance from gravicenter in equatorial radii
- $\phi$  = gravicenter latitude

In an analysis of the perturbations of the bound orbit of an Earth satellite, it is necessary to consider several of the harmonic terms to describe accurately the motion of the vehicle over an extended period of time (Ref. 6 and 7). However, only the second harmonic  $J_2$  contributes significantly to the perturbations of the elements of a non-bound or hyperbolic orbit, since the time spent in the vicinity of the planet is short and the effects of the higher order harmonics are negligible.

The perturbing potential  $R$  due to the second harmonic  $J_2$  is given by

$$R = U - \frac{k^2}{r} = -J_2 \frac{k^2}{r^3} P_2(\sin \phi) \quad (2)$$

where

$$P_2(\sin \phi) = \frac{1}{2}(3 \sin^2 \phi - 1) \quad (3)$$

The distance from the gravicenter  $r$  and gravicenter latitude  $\phi$  expressed as functions of the osculating elements of the vehicle are

$$r = p/(1 + e \cos \nu) \quad (4)$$

and

$$\sin \phi = \sin i \sin(\omega + \nu) \quad (5)$$

where

- $p = h^2/k^2 = (-a)(e^2 - 1)$  = semilatus rectum
- $a$  = semitransverse axis
- $h$  = angular momentum
- $e$  = eccentricity
- $i$  = inclination to the equatorial plane
- $\omega$  = argument of perigee
- $\nu$  = true anomaly

The disturbing function  $R$ , when expressed in terms of the osculating elements of the orbit, becomes

$$R = J_2(k^2/2p^3)(1 + e \cos \nu)^3 \left[ 1 - \frac{3}{2} \sin^2 i + \frac{3}{2} \sin^2 i \cos(2\omega + 2\nu) \right] \quad (6)$$

## III. VARIATION OF ORBITAL ELEMENTS

The solution of the differential equations representing the variations of the orbital elements with respect to time is derived by a method analogous to that employed by Kozai (Ref. 8) in investigations of elliptic motion. The orbital elements  $E$ ,  $h$ ,  $h_z$ ,  $\tau$ ,  $\omega$ , and  $\Omega$  are employed, since they both form a canonical set and are also well behaved for eccentricities near unity. The elements not previously defined are

$$E = -k^2/2a = \text{undisturbed energy}$$

$$h_z = h \cos i = \text{component of angular momentum along polar axis}$$

$$\tau = \text{time of perifocal passage}$$

$$\Omega = \text{longitude of the ascending node}$$

The rate of change of the orbital elements with time may be expressed in terms of the differential coefficients of  $R$  as

$$d\tau/dt = -\partial R/\partial E \quad (7)$$

$$dE/dt = \partial R/\partial \tau \quad (8)$$

$$d\omega/dt = -\partial R/\partial h \quad (9)$$

$$dh/dt = \partial R/\partial \omega \quad (10)$$

$$d\Omega/dt = -\partial R/\partial h_z \quad (11)$$

$$dh_z/dt = \partial R/\partial \Omega \quad (12)$$

Since the orbital elements of the vehicle change only slightly due to the effects of the oblateness, the perturbations of the first order may be derived by considering the elements appearing in  $R$  on the right side of Eq. (7) through (12) constant. If the elements are assumed constant, the true anomaly may be regarded as a known function of time, and the independent variable may be transformed from time to the true anomaly by

$n(t - \tau)$ , where the mean motion  $n$  is a function of the element  $E$  through the harmonic law  $n = (2E)^{3/2}k^{-2}$ . The variable  $M$  corresponds to the mean anomaly for hyperbolic motion and is a function of both the true anomaly and the eccentricity, and hence the disturbing function involves the element  $h$  both explicitly and also implicitly through the true anomaly.

Since an axially symmetric density distribution is assumed, the disturbing function  $R$  is independent of  $\Omega$ , and Eq. (12) becomes

$$dh_z/dt = 0 \quad (14)$$

and

$$h_z = h_z(0) = \text{const} \quad (15)$$

the component of angular momentum along the polar axis being unaffected by the oblateness.

The perturbations of the remaining five orbital elements are given in Eq. (16) through (20) where  $M$  and  $n$  appearing in Eq. (20) are the mean anomaly and mean motion, respectively. These expressions for the perturbations are to be evaluated between the limits  $\nu_0$  and  $\nu$ .

$$\delta E = R \Big|_{\nu_0}^{\nu} \quad (16)$$

$$\delta h = J_2 \frac{h \sin^2 i}{4p^2} \left[ 3e \cos(2\omega + \nu) + 3 \cos(2\omega + 2\nu) + e \cos(2\omega + 3\nu) \right] \Big|_{\nu_0}^{\nu} \quad (17)$$

$$\delta \Omega = -J_2 \frac{\cos i}{4p^2} \left\{ 6(\nu + e \sin \nu) - [3e \sin(2\omega + \nu) + 3 \sin(2\omega + 2\nu) + e \sin(2\omega + 3\nu)] \right\} \Big|_{\nu_0}^{\nu} \quad (18)$$

$$\begin{aligned} \delta \omega + \cos i \delta \Omega = J_2 \frac{3}{2p^2} \left\{ \left( 1 - \frac{3}{2} \sin^2 i \right) \left( \nu + \frac{4 + 3e^2}{4e} \sin \nu + \frac{1}{2} \sin 2\nu + \frac{e}{12} \sin 3\nu \right) - \right. \\ \left. \frac{\sin^2 i}{48e} \left[ 3e^2 \sin(2\omega - \nu) + (12 - 21e^2) \sin(2\omega + \nu) - 36e \sin(2\omega + 2\nu) - \right. \right. \\ \left. \left. (28 + 11e^2) \sin(2\omega + 3\nu) - 18e \sin(2\omega + 4\nu) - 3e^2 \sin(2\omega + 5\nu) \right] \right\} \Big|_{\nu_0}^{\nu} \quad (19) \end{aligned}$$

$$\begin{aligned} \delta \tau + \frac{(e^2 - 1)^{1/2}}{n} (\delta \omega + \cos i \delta \Omega) = J_2 \frac{3(e^2 - 1)^{1/2}}{2np^2} \left\{ \left( 1 - \frac{3}{2} \sin^2 i \right) (\nu + e \sin \nu) + \right. \\ \left. \frac{1}{4} \sin^2 i [3e \sin(2\omega + \nu) + 3 \sin(2\omega + 2\nu) + e \sin(2\omega + 3\nu)] + \frac{3MR}{n^3 a^2} \right\} \Big|_{\nu_0}^{\nu} \quad (20) \end{aligned}$$

$$d/dt = h/r^2 \quad d/d\nu \quad (13)$$

The disturbing function involves the element  $E$  and  $\tau$  implicitly through the true anomaly from the relation  $M =$

The perturbations of the semitransverse axis  $a$ , eccentricity  $e$ , and orbital inclination  $i$  are found from

$$\delta a = k^2/2E^2 \delta E \quad (21)$$

$$\delta e = \frac{(e^2 - 1)}{2e} \left( \frac{\delta E}{E} + 2 \frac{\delta h}{h} \right) \quad (22)$$

$$\delta i = \cot i (\delta h/h) \quad (23)$$

The expressions for the variations of the elements  $E$ ,  $h$ ,  $h_z$ , and  $\Omega$  are well behaved for eccentricities near unity; however, the expression for the variation of the time of perifocal passage  $\tau$  breaks down when  $e = 1$ . Fortunately, in most cases of interest, the change in the time of perifocal passage is of not great importance.

Of additional importance in the analysis of interplanetary escape trajectories is the velocity vector of the vehicle at a great distance from Earth. The magnitude of this hyperbolic excess velocity vector is given by the following function of the energy:

$$V_h = (2E)^{1/2} \quad (24)$$

The unit vector  $S$  in the direction of the hyperbolic excess velocity vector and also in the direction of the outgoing asymptote of the hyperbola has direction cosines of the form

$$S_1 = \cos \phi_h \cos \alpha_h = \cos \Omega \cos (\omega + \nu_h) - \sin \Omega \sin (\omega + \nu_h) \cos i \quad (25)$$

$$S_2 = \cos \phi_h \sin \alpha_h = \sin \Omega \cos (\omega + \nu_h) + \cos \Omega \sin (\omega + \nu_h) \cos i \quad (26)$$

$$S_3 = \sin \phi_h = \sin (\omega + \nu_h) \sin i \quad (27)$$

$\alpha_h$  and  $\phi_h$  being the right ascension and declination of the hyperbolic excess velocity vector and  $\nu_h$  being the angle between the hyperbolic excess velocity vector and periapsis.

The angle  $\nu_h$  is related to the eccentricity of the hyperbola by

$$\cos \nu_h = -1/e \quad (28)$$

The perturbation of the magnitude of the hyperbolic excess velocity vector is given by

$$\delta V_h = \delta E/V_h \quad (29)$$

whereas the perturbations of the right ascension and declination are given by

$$\delta \alpha_h = \delta \Omega - \frac{\sin \phi_h \cos (\omega + \nu_h)}{\cos^2 \phi_h} \delta i + \frac{\cos i}{\cos^2 \phi_h} (\delta \omega + \delta \nu_h) \quad (30)$$

$$\delta \phi_h = \frac{\cos i \sin (\omega + \nu_h)}{\cos \phi_h} \delta i + \frac{\sin i \cos (\omega + \nu_h)}{\cos \phi_h} (\delta \omega + \delta \nu_h) \quad (31)$$

The perturbation of the angle between  $S$  and periapsis is given by

$$\delta \nu_h = (\cos^2 \nu_h / \sin \nu_h) \delta e \quad (32)$$

#### IV. EXAMPLE OF AN EARTH-ESCAPE MISSION

As an example of the application of the derivation of the perturbations, an Earth-escape mission with the initial parameters shown in Table 1 was used. The perturbations of the elements  $a$ ,  $e$ ,  $i$ ,  $\tau$ ,  $\omega$ , and  $\Omega$  were calculated from Eq. (16) through (20) and are shown in Fig. 1 through

6 as functions of the true anomaly. The time along the trajectory may be determined from Fig. 7 as a function of the true anomaly. The maximum true anomaly is approximately 2.5 rad; in the following discussion the time of 240 min corresponds to a true anomaly of about 2.3 rad.



**Table 1. Example of an Earth-escape mission**

Trajectory parameters	
$k^2, \text{km}^3/\text{sec}^2$	$0.398602 \times 10^6$
$r_r, \text{km}$	6378.150
$J_2$	$1.08228 \times 10^{-3}$
$J_3$	$-0.00230 \times 10^{-3}$
$J_4$	$-0.00212 \times 10^{-3}$
Initial position and velocity	
$X, \text{km}$	3826.8900
$Y, \text{km}$	-4418.9120
$Z, \text{km}$	-2551.2600
$\dot{X}, \text{km/sec}$	9.4864475
$\dot{Y}, \text{km/sec}$	6.1616282
$\dot{Z}, \text{km/sec}$	3.5574179
Initial osculating elements	
$a, \text{km}$	-25,512.6000
$e$	1.25000000
$\tau, \text{sec}$	0.0
$i, \text{rad}$	0.52359881
$\omega, \text{rad}$	5.35589010
$\Omega, \text{rad}$	0.0

selected points along the path, the osculating elements were calculated and the perturbations of the initial elements determined. These values are shown as individual points in Fig. 1 through 6. In the numerical integration the second, third, and fourth harmonic terms were retained in the potential function. The values of these coefficients are shown in Table 1 and correspond to the following values for the commonly used coefficients for the second, third, and fourth zonal harmonics:

$$J = 1.62341 \times 10^{-3}$$

$$H = -0.00604 \times 10^{-3}$$

$$K = 0.00637 \times 10^{-3}$$

The asymptotic values of the elements for  $t \rightarrow \infty$  are shown in Table 2. In addition, the asymptotic values for the perturbations of the hyperbolic excess velocity vector are shown in Table 3.

**Table 2. Asymptotic value of the orbital elements**

$a, \text{km}$	-25,570.033
$e$	1.24951297
$\tau, \text{sec}$	0.160659
$i, \text{rad}$	0.52367376
$\omega, \text{rad}$	5.35710409
$\Omega, \text{rad}$	-0.00047714

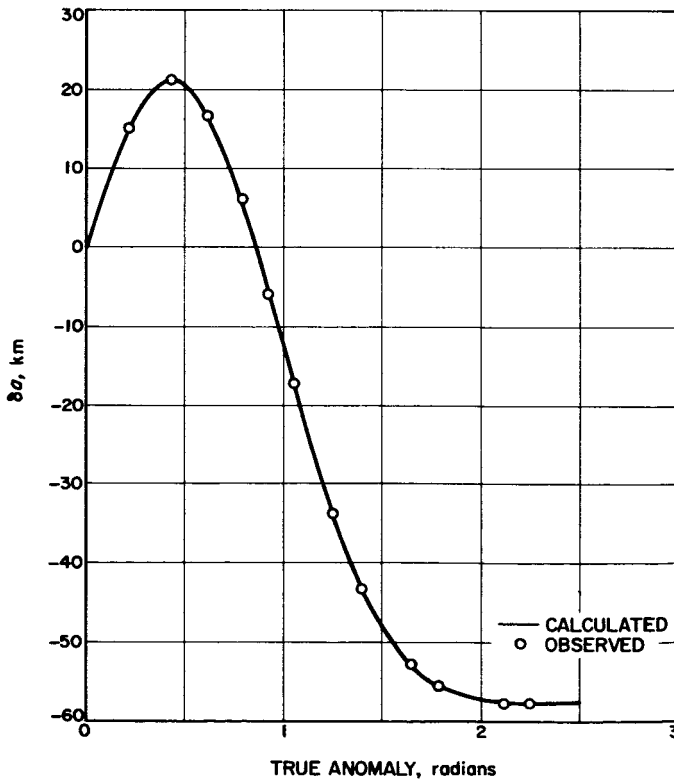


**Fig. 1. Perturbation of the semi-transverse axis**

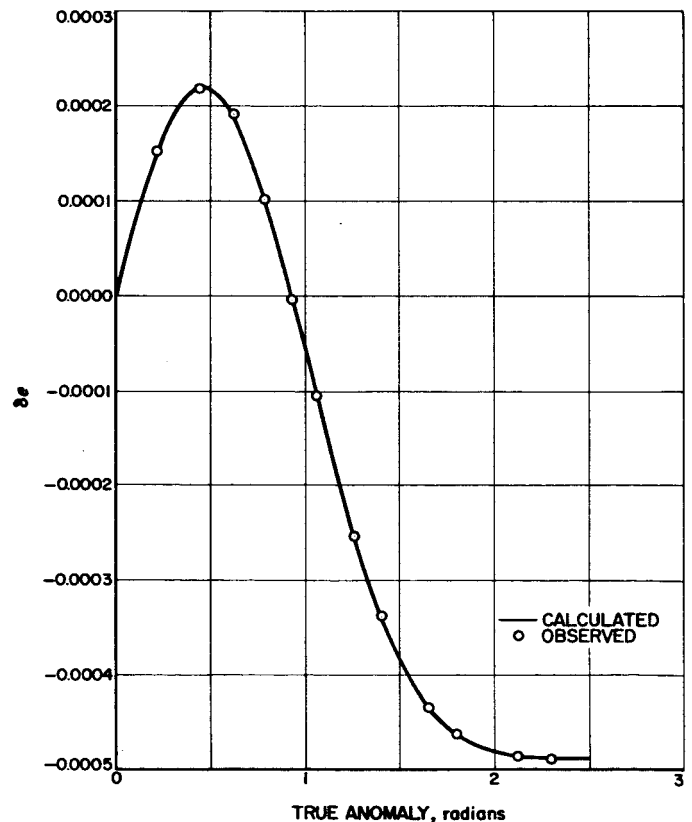


**Fig. 2. Perturbation of the eccentricity**

To check the results that were obtained, a numerical integration of the equations of motion was performed. At

An indication of the accuracy of the analysis calculation of the perturbations may be had by observing the calculated and observed perturbations of the orbital elements at  $t = 240$  min in Table 4. An observation of the variation

**Table 3. Asymptotic perturbations of the hyperbolic excess velocity vector**

$\delta V_h$ , km/sec	0.004449
$\delta a_h$ , rad	$1.52565 \times 10^{-3}$
$\delta \phi_h$ , rad	$0.07498 \times 10^{-3}$

**Table 4. Calculated and observed perturbations at 240 min**

Perturbed element	Observed value, numerical int.	Calculated value, 1st iteration	Calculated value, 2nd iteration
$\delta a$ , km	-57.713	-57.387	-57.729
$\delta e$	-0.0004887	-0.0004868	-0.0004876
$\delta \tau$ , sec	0.1660	0.1635	0.1699
$\delta i$ , mrad	0.07499	0.07558	0.07501
$\delta \omega$ , mrad	1.2100	1.2076	1.2071
$\delta \Omega$ , mrad	-0.4695	-0.4683	-0.4678

of the elements in Fig. 1 through 6 would indicate that the initial osculating elements are not necessarily the best to

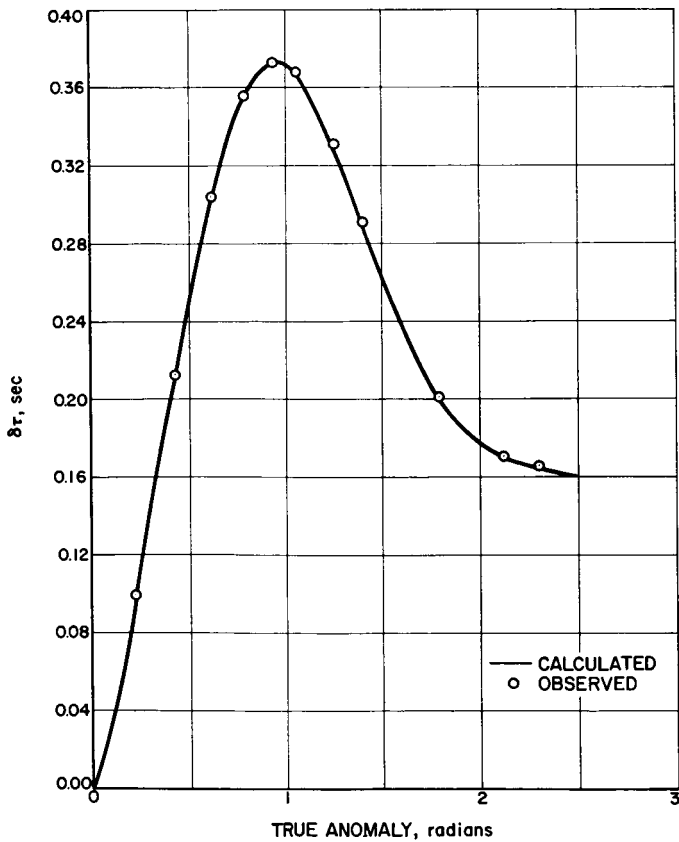


**Fig. 3. Perturbation of the time of peri-focal passage**

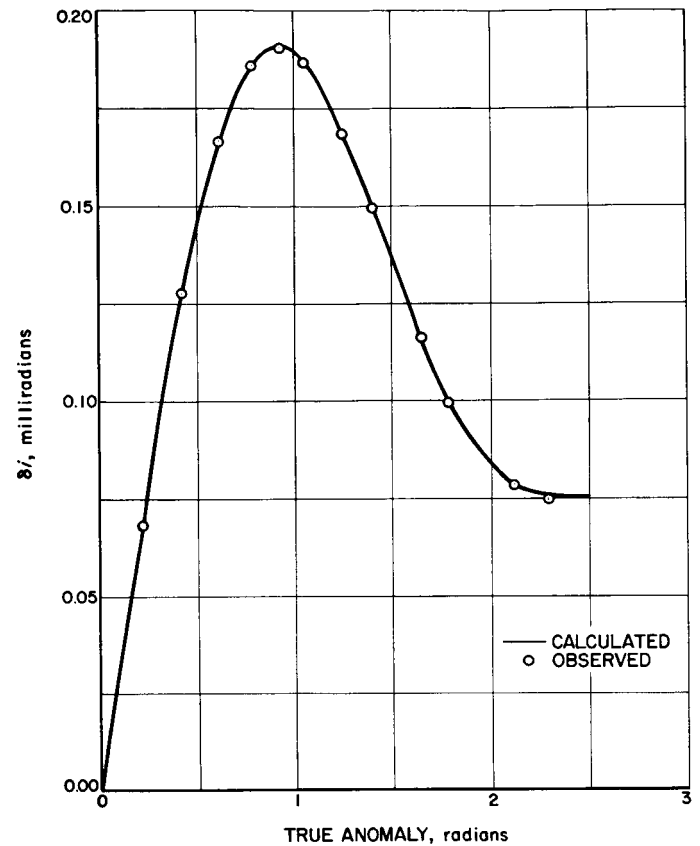


**Fig. 4. Perturbation of the inclination**

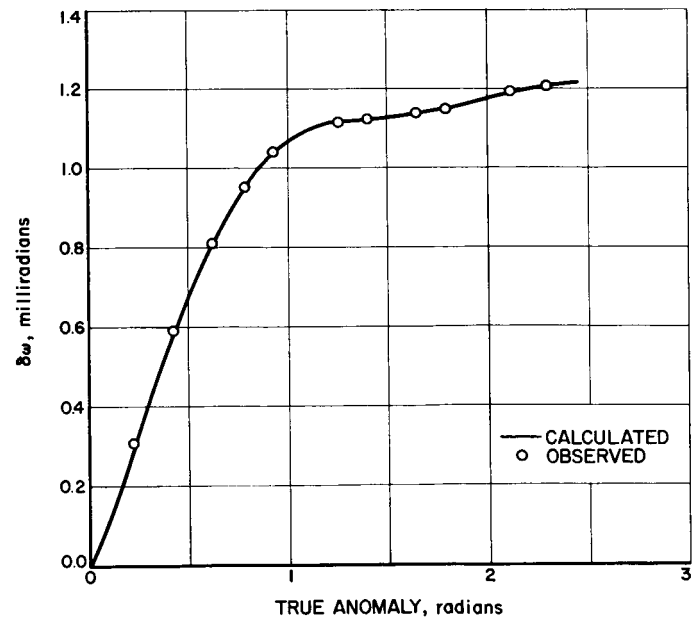


**Fig. 5. Perturbation of the argument of perigee**

**Table 5. Position and velocity at  $T = 240$  min**

Coordinate	Observed value, numerical int.	Calculated value, 2nd iteration	Unperturbed value
X, km	16,781,044	16,781.333	16,876.470
Y, km	72,067.631	72,067.541	72,092.005
Z, km	41,620.015	41,619.951	41,622.339
$\dot{X}$ , km/sec	0.098739	0.098754	0.105018
$\dot{Y}$ , km/sec	4.327236	4.327235	4.329987
$\dot{Z}$ , km/sec	2.498790	2.498790	2.499919

use in the expressions for the perturbations. If a second iteration is made in which the elements used in calculating the perturbations are the asymptotic values from Table 2, then slightly better values are realized for the perturbations as shown in Table 4. A comparison between the results of the second iteration and the numerical integration in the position and velocity of the vehicle at  $t = 240$  min is shown in Table 5. Also shown in Table 5 are the unperturbed values of position and velocity at 240 min.

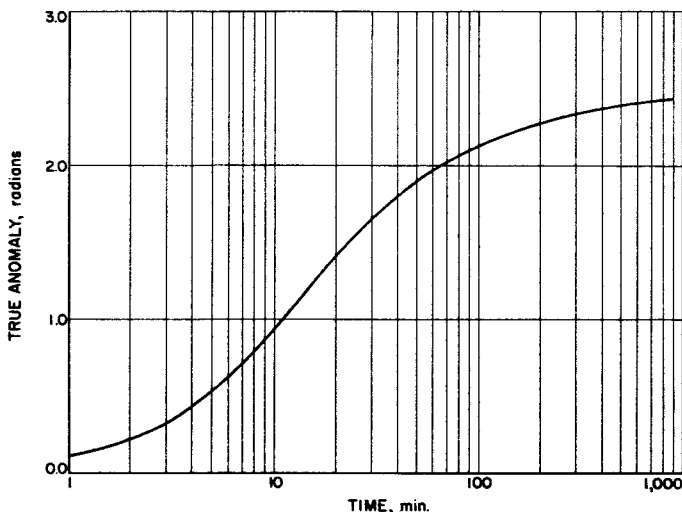


**Fig. 6. Perturbation of the longitude of the ascending node**

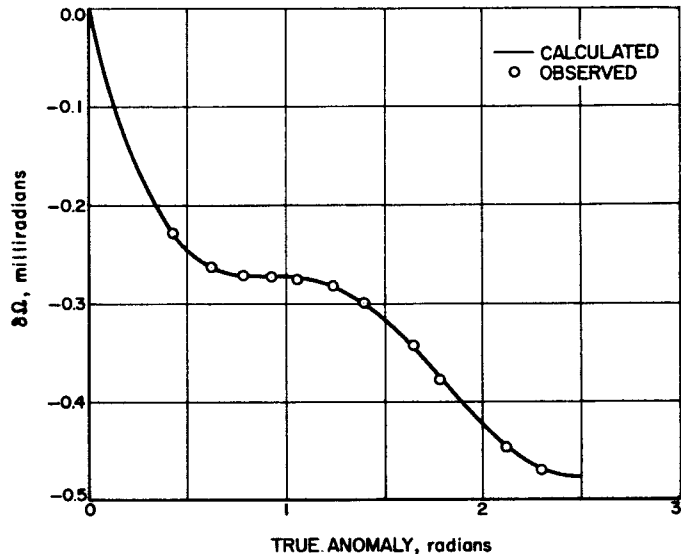


**Fig. 7. True anomaly vs time ( $e = 1.25$ )**

## REFERENCES

1. Anthony, M. L., and G. E. Fosdick, "Escape in the equatorial plane of an oblate planet," *ARS Journal*, 30, 898-900, 1960.
2. Anthony, M., G. Fosdick, and L. Perko, "Escape from an oblate planet," *Advances in the Astronautical Sciences*, vol. 7, p. 175. Plenum Press Inc., New York, 1961.
3. Hori, Gen-Ichiro, "The motion of hyperbolic artificial satellite around the oblate earth," *Astronomical Journal*, 66, 258-263, 1961.
4. Bomford, B. G., *Geodesy*, Clarendon Press, Oxford, 1952, Chap. 7.
5. Garfindel, B., "The orbit of a satellite of an oblate planet," *Astronomical Journal*, 64, 353-367, 1959.
6. Brouwer, D., "Solution of the problem of artificial satellite theory without drag," *Astronomical Journal*, 64, 378-397, 1959.
7. O'Keefe, J. A., A. Eckels, and R. K. Squires, "The gravitational field of the earth," *Astronomical Journal*, 64, 245-253, 1959.
8. Kozai, Y., "The motion of a close earth satellite," *Astronomical Journal*, 64, 367-377, 1959.